On the use of thermographic technique to assess the fatigue performance of bonded joints

C.F.C. Bandeira, P.P. Kenedi, L.F.G. Souza, Silvio DE BARROS

On the Use of Thermographic Technique to Assess the Fatigue Performance of Bonded Joints

C.F.C. Bandeira[a], P.P. Kenedi[a], L.F.G. Souza[a], S. de Barros[a,b,*]

[a]Federal Center of Technological Education of Rio de Janeiro – CEFET/RJ, Av. Maracanã, 229, Rio de Janeiro/RJ, Brazil
[b]Université de Nantes, Institut de Recherche en Génie Civil et Mécanique, Saint-Nazaire, France

ABSTRACT

The thermographic technique is based on the heat released during dynamic loading cycles, correlating the temperature variation on specimen's surface with the applied stress amplitude. An abrupt temperature variation under a specific stress level reveals the presence of an irreversible phenomenon inside the material, which could be associated with fatigue damage process. In this work, the fatigue performance of bonded joints is assessed by carrying out fatigue tests in a servo-hydraulic machine monitored continuously by a thermographic acquisition system, with the utilization of end notched flexure specimens composed by two steel plates of ASTM A36, bonded together with epoxy adhesive. The results confirm that the thermographic technique is quite promising as an alternative approach to estimate the bonded joint fatigue strength.

Keywords: durability, fatigue, joint design, thermography.

1. INTRODUCTION

The fatigue performance is a very important issue in design of structures submitted to dynamic loading. The fatigue of bonded joints has been studied by many authors in order to understand what happens with substrates and adhesive when they are subjected to variable loading [1-6].

Abdel Wahab [7] did an extensive review of fatigue in adhesively bonded joints, defining two main approaches for fatigue analysis: stress-life and fatigue crack initiation/propagation. In fact, according to the author, there is a clear search to find a fatigue threshold for materials, as a fatigue limit; however, this is not the case for adhesively bonded joints and the fatigue threshold for this type of structures is usually specified at a certain number of cycles, for instance, one million cycles. For fatigue crack initiation, damage models can be used, based on empirical assumptions, as the

*Corresponding author: E-mail address: silvio.debarros@gmail.com

models of plastic or principal strains, or based on scientific observations, as the models related to the theory of continuum damage mechanics. For fatigue crack propagation, the idea is to combine a fracture parameter, such as strain energy release rate (G) and the crack growth rate (da/dN) using fracture mechanics tests.

Chaves *et al*. [8] did an interesting review of fracture mechanics tests for adhesively bonded joints. The characterization of adhesive joints fracture was divided in three basic approaches: continuum mechanics, fracture mechanics and damage mechanics. In the continuum mechanics approach, stresses and deformations of the bonded parts were described to define the maximum force that can be applied to the joint in four different loading types: normal, shear, peeling and cleavage. The fracture mechanics assumes the material non-continuity, recognizing delamination, debonding, cracking and other imperfections. Indeed, fracture mechanics can be divided into two basic approaches: stress intensity factor criterion and energetic criterion. The energetic criterion has been more utilized in adhesive joints and is based on the comparison between the strain energy release rate (SERR) and the critical energy value (G_{Ic}), which is a material characteristic. Even the damage mechanics is divided in continuum damage models (CDM) and cohesive zone models (CZM), which a geometric interpretation is shown in Fig.1, as in Chaves *et al*. [8], where the area inside the lines is the value of G_{IIc} (G_c in shear loading mode).

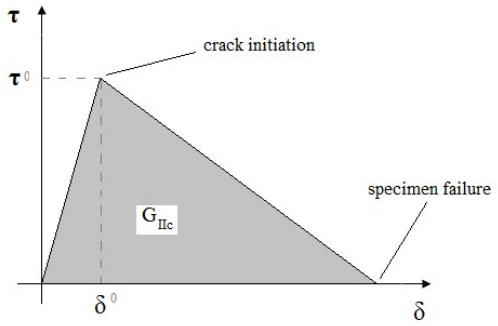

Figure 1 – Bilinear cohesive law (Chaves *et al.* [8] – adapted).

Blackman *et al*. [9] used Linear Elastic Fracture Mechanics (LEFM) to estimate values of the mode II adhesive fracture energy for bonded joints, through the utilization of various forms of beam theory corrections. Also, the concept of an effective crack length was introduced and then used to calculate corrected values of G_{IIC}. Romanos *et al*. [10] presents a stress-life approach to predict fatigue properties of adhesively bonded joints by using structural adhesives. A butt-bonded hollow cylinders test procedures

based upon ISO 11003-1 [11] have been used, with a torsion test, to provide a very uniform shear stress in the adhesive layer with negligible variation across the adhesive ring. The article intended to prove the transferability of fatigue data evaluated using standard specimens, to bonded structures and components tested in fatigue.

Allen *et al*. [12] proposed that only using the Wohler approach, which is expensive and time consuming, it could be checked if fatigue limit of bonded joints exists or not. On the other hand, it was proposed the utilization of Prot [13] approach to do an estimative of fatigue limit without explicitly addressing the correspondent number of cycles.

De Barros *et al*. [14] studied the influence of mechanical surface treatment on fatigue of bonded joints, running fatigue tests on three-point bending fixture. End notched flexure specimens composed by two plates of steel ASTM A36 bonded together with the adhesive Novatec Primer NVT-1 were used. Three different surface treatments were considered for substrate: sand blasting, grit blasting and bristle blasting. It was observed that mechanical surface treatment has much influence on fatigue behaviour of bonded joints, which is not so characteristic in static loading condition. Grit and sanding blasting presented higher fatigue performance compared to the bristle one, having a fatigue life overcoming 10^6 cycles under 50% of loading level (applied load / load which the substrate yields).

In this article, the fatigue performance of bonded joints is assessed using the thermographic technique proposed by Risitano [15], which is also considered an accelerated method as the one proposed by Prot [13]. Specimens, as used in Barros *et al*. [14] with sanding blasting surface treatment, were tested under three-point bending fixture, monitored continuously by an infrared camera. To define the fatigue performance of bonded joints, the nomenclature used in the ASTM D3166-99 [16] was adopted: adhesive joint fatigue strength, which address the situation where it is considered that the adhesive joint has reached a limit condition of crack initiation process could occur.

2. EXPERIMENTAL METODOLOGY

In this section, a brief description of the thermographic technique and all experimental resources used in the development of this research are presented.

2. THERMOGRAPHIC TECHNIQUE

The thermographic technique is mainly characterized by the use of thermo elasticity principles, through the measurement of the temperature variation on the external surface of specimens during variable loading application. It is known that a body subjected to variable loading experiences a changing on its temperature, where irreversible damage can be produced in material for larger temperature variation. This approach can be used to assess the fatigue behaviour of materials, proposing the hypothesis that fatigue failure occurs when the plastic deformation energy reaches a constant value (E_c), characteristic of each material, as in Fargione *et al.* [17] and Risitano *et al*. [15]. This assumption allowed a prompt correlation between the temperature increasing and the number of loading cycles, since fatigue damage is an energy dissipation process, as in Hou *et al*. [18]. Figure 2 shows, schematically, the temperature behaviour (T) on specimen surface during fatigue cycles (N) under a loading amplitude large enough to initiate and propagate cracks.

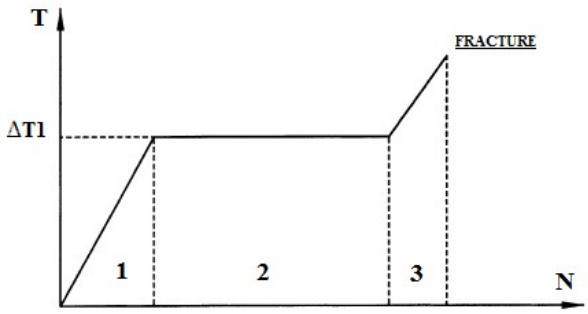

Figure 2– Relationship $\boldsymbol{T}$ vs $\boldsymbol{N}$ during fatigue loading.

Figure 2 schematically shows the three thermal phases (1, 2 and 3), which could be associated, respectively, with crack initiation, crack propagation and unstable failure process. The temperature variation of phase 1 (ΔT_1) increases as higher is the loading level relatively to the material fatigue strength (FS). Although Fig. 2 shows no temperature variation ($\partial T/\partial N_2 = 0$) in phase 2, there are also materials with a temperature increasing rate constant. This phase is responsible for the majority of test cycles. Finally, the number of cycles spent in phase 3 is relatively small if compared to others phases because the damage is quite significative culminating in unstable crack

growth. The temperature in this last phase can reach more than 100 ºC depending on the material and loading level tested.

Risitano [15] proposed to determine the temperature variation (ΔT) for only phase 1, in homogeneous materials, since it can represent the crack initiation process, for different stress amplitude (σ_a) in order to obtain the relationship ΔT_1 x σ_a. This relation has a bilinear profile with different slopes $d(\Delta T_1)/d\sigma_a$, characterizing a transition region from no fatigue damage (lower slope) to fatigue damage (higher slope). With this relation, the material fatigue limit can be determined (for materials, as ferrous alloys, which present this behaviour) by the extension of the straight line with higher slope until it across σ_a-axis, where $\Delta T_1 = 0$, representing no crack initiation and, consequently, no perceptible fatigue damage process. In the present work, there is an adaptation of this process, instead of using a ΔT_1 x σ_a graphic used for homogenous materials it was used ΔTx Q % graphics (shown in Figures 10 and 11) adapted to non-homogeneous materials, where Q % is defined as a relation of the applied load in three points bending fixture and the load that begging to yield the substrate.

2.2 EXPERIMENTAL APPARATUS

Three specimens (SP) were submitted to fatigue tests in a servo hydraulic machine, using a three-point bending fixture. Sinusoidal loading was used with a frequency $f = 20Hz$ and a loading ratio of $R = P_{min}/P_{max} = 0.1$, where P is the applied transversal load. Figure 3 shows a specimen on the testing fixture and its main dimensions.

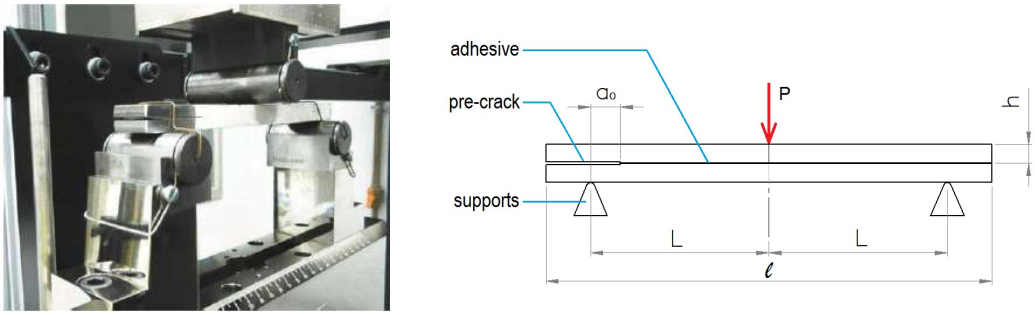

(a) (b)

Figure 3 – Specimen: (a) on the three points bending fixture and (b) main dimensions.

The specimen dimensions are the same used in de Barros *et al*. [14], with pre-crack length a_0 = 25 mm, width b = 25 mm, total length l = 190 mm and substrate thickness h = 6 mm. The distance between lower and upper rollers was stated as L = 80 mm. The adhesive used was the Novatec Primer NVT-1, semi-flexible epoxy-based adhesive (epoxy+polyamine) with polymerization time of two hours, with high abrasion resistance, anticorrosion protection and high adhesion, with 0.5 mm thickness. In order to guarantee thickness of the adhesive, spacers were used. Also, polypropylene plastics, with waxed surfaces, were used to form the pre-crack length.

Table 1 provides material mechanical properties of the cured adhesive.

Table 1: Mechanical properties of cured adhesive Novatec Primer NVT-1

Mechanical Property	**Value**
Ultimate strength, MPa	27
Hardness,Shore D	60

The fatigue loading was applied as a percentage of the load necessary to yield the substrate (F_y = 6293 N), as in de Barros *et al*. [14]. The first specimen (SP_1) was tested under only one level of sinusoidal fluctuating loading to determine the three thermal phases of the bonded joint and the approximate number of cycles necessary to define the phase 1 (N_1). Second (SP_2) and third (SP_3) specimens were tested under different levels of sinusoidal fluctuating loadings, each one during the number of cycles (N_1) obtained with (SP_1). Table 2 shows the fatigue loading $Q\ \% = (P/F_y)\cdot 100\%$, for each specimen.

Table 2: Fatigue loading for each specimen.

SP	**Q %**
1	80
2	30, 40, 50, 60, 70, 80, 90
3	10, 20, 30, 40, 50, 60, 70, 80

All fatigue tests were continuously monitored by an infrared camera FLIR® A320 with 320x240 pixels resolution, data acquisition frequency of 30 Hz and temperature sensitivity equal to 30 mK. Movies were recorded for each specimen and post processed by ResearchIR® software from FLIR. In order to improve camera performance, all specimens were painted with black ink on its lateral surface and a black cloth was used to cover test apparatus, besides all lights and air conditioner have

been turned off to minimize any spurious thermal effects that could interfere with the temperature measurement. Figure 4 shows camera under black cloth and the specimen painted with black ink.

(a) (b)

Figure 4 – (a) camera under black cloth; (b) specimen painted with black ink.

The specimen's surface temperature was monitored from the pre-crack tip to the half specimen, since it is expected that region to be the most critical one. A rectangular area was defined around it, as shown in Fig. 5. Inside this area, during fatigue loading cycles, was registered the maximum temperature (T_{max}) by the infrared camera.

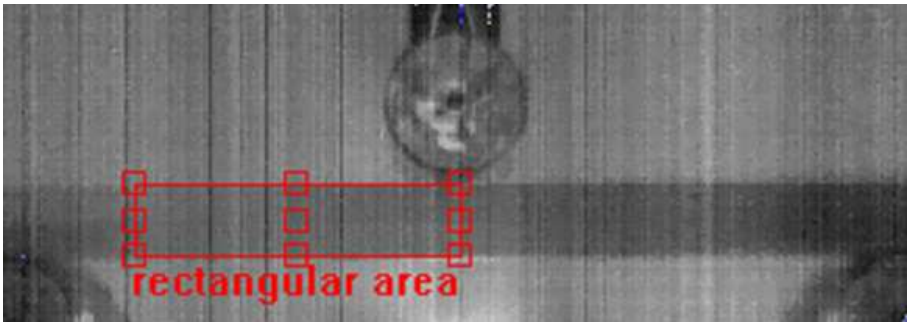

Figure 5 – Rectangular area.

The next section presents the results obtained for each specimen and the adhesive joint fatigue strength determined by Risitano approach [15].

3. RESULTS

The maximum temperature was obtained around crack tip as evidenced by images from ResearchIR® software. During loading cycles, it was possible to verify temperature gradients in this region. Figure 6 shows the temperature distribution into rectangular area during SP_3 test, for different loading levels.

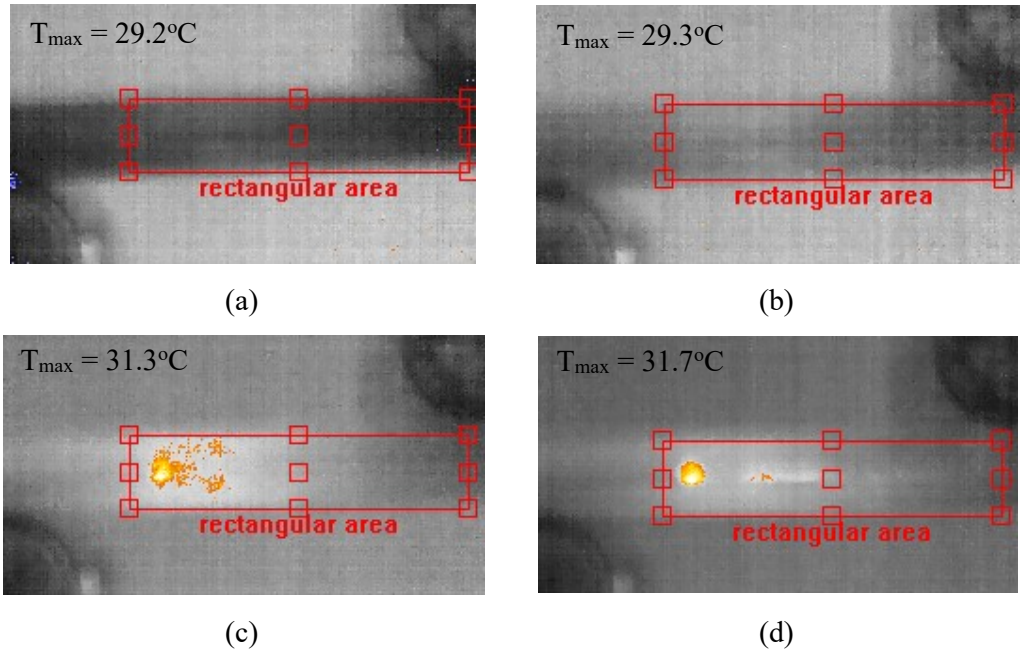

Figure 6 – Temperature distribution during SP_3 test: (a) Q = 60%; (b) Q = 70%; (c) Q = 80% (close to failure); (d) Q = 80% (just after the failure moment)

Figure 6 shows that maximum temperature distribution that experientially occurs next to pre-crack tip, concentrating energy release in this region. In addition, Figure 6.d shows just after the failure moment, the highest temperature (T_{max} = 31.7 ºC) is located at pre-crack tip region, represented by the multi-colored circle.

The first specimen was tested until failure under only one level of sinusoidal fluctuating loading Q = 80%. The maximum temperature on its lateral surface during all fatigue loading cycles is shown in Fig. 7.

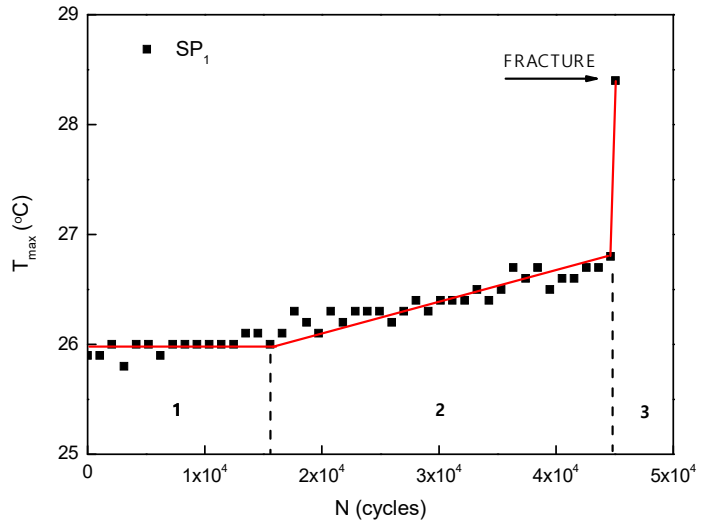

Figure 7 – Relationship T_{max} x N for SP_1.

Figure 7 shows the thermal phases 1, 2 and 3 of the bonded joint. It can be noted that first phase has a very small temperature variation until reaches N_1~ 16,000 cycles, when starts phase 2. This second phase has a maximum temperature increasing rate ($\partial T_{max}/\partial N$) different than zero and is responsible for the majority of loading cycles. As expected, the last phase shows a considerable temperature variation compared to the others due to the unstable crack propagation to final fracture which releases more heat. Note that third phase was recorded by only one frame acquisition, just after the failure moment, as shown by the single point plotted in Fig. 7. This happened due the relatively low sample rate of the thermic data acquisition system. Also after the instable crack propagation event, that are prone to occur in the ENF test [19, 20], the specimen stiffness suddenly dropped down, activating the testing machine interlock, that stopped the test. So that single point represents the maximum temperature acquired just after the instable crack propagation has occurred.

The maximum temperature evolution observed on SP_1 has a temperature variation of about ΔT_{max} = 3 ºC, being 2 ºC associated to the final fracture at $N \approx$ 45,000 cycles. This temperature variation is very small if compared with other materials, which may reach ΔT_{max}>100 ºC in some cases, that can be explained by larger values of specific mass and specific heat when compared to adhesively bonded joints.

The second (SP_2) and the third (SP_3) specimens were tested according to Risitano proposal, under different levels of sinusoidal fluctuating loadings Q defined at Table 2, only for a few number of cycles required to reach the second thermal phase defined in the SP_1 test, N_1~ 16,000 cycles. However, in order to ensure that at each loading, the phase I was really terminated before it was considered the beginning of second thermal phase, it was decided to use N_1 = 20,000 cycles instead of 16,000 cycles.

Figures 8 and 9 show the maximum temperature on the lateral surface of specimens SP_2 and SP_3, respectively, for each loading level presented at Table 2.

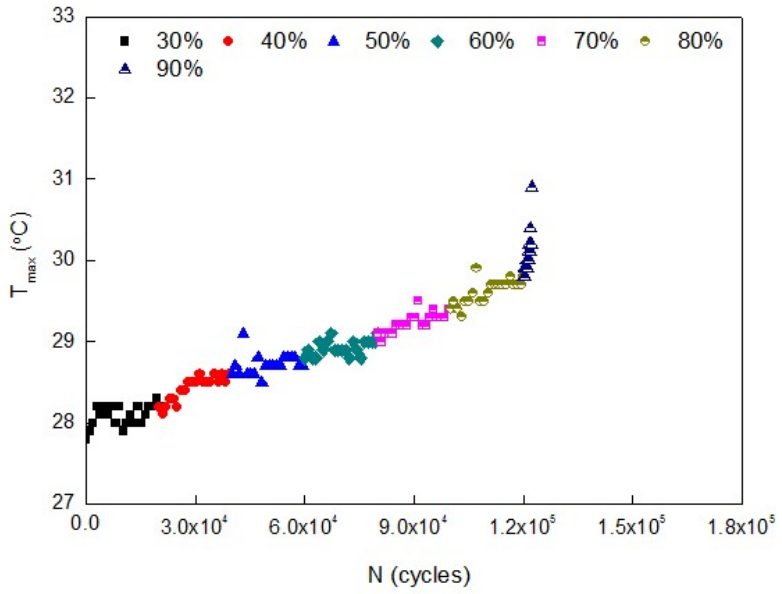

Figure 8 – Relationship T_{max} x N for SP_2.

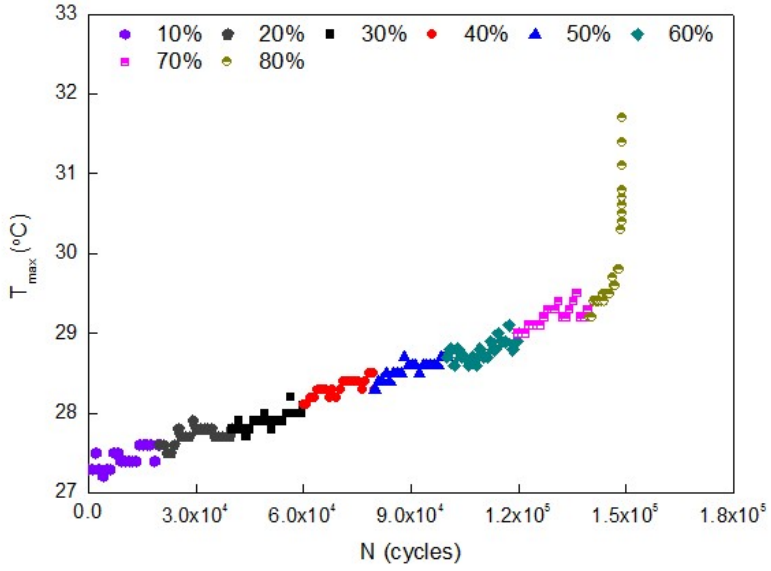

Figure 9 – Relationship T_{max} x N for SP_3.

Temperature variations were most pronounced always on the last loading level due to the final fracture (crack unstable propagation). Note that SP_2 started from Q = 30% while SP_3 started from Q = 10%, to improve third specimen results. In addition, while SP_2 failed under Q = 90%, and SP_3 failed under Q = 80%.

To estimate the bonded joint fatigue strength, it was plotted the relationship ΔT x Q for both specimens. Then FS is obtained by fitting a straight line through higher ΔT values, using least squares method, and extending the straight line until reach Q-axis, where ΔT = 0. Figures 10 and 11 show the relationship ΔT x Q and fitted lines for specimens SP_2 and SP_3, respectively.

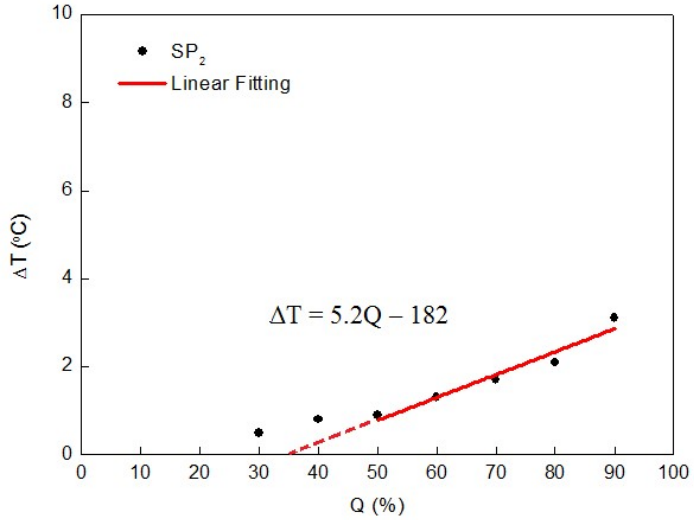

Figure 10 - ΔT x Q for SP_2

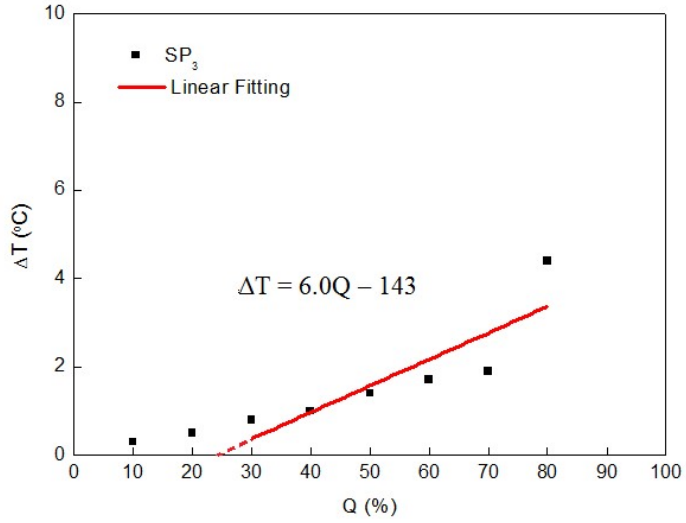

Figure 11 - ΔT x Q for SP_3

Table 3 shows the fitting line equation for each specimen, Q value for $\Delta T = 0$ and the estimative of average (μ_{FS}) for the adhesive joint fatigue strength.

Table 3: Fitting line parameters and adhesive joint fatigue strength calculation.

Specimen	**Fitting line**	**Q ($\Delta T = 0$)**	**μ_{FS}(%)**
SP_2	$\Delta T = 5.2Q - 182$	35.0	29.4
SP_3	$\Delta T = 6.0Q - 143$	23.8	

Table 3 shows that FS average is around 30%. In addition, even considering the highest value for adhesive joint fatigue strength, it would be lower than the minimum load level Q = 50% tested in de Barros *et al*. [14] that did not fail sand blasting specimens after reaching more than $1 \cdot 10^6$ cycles, meaning that thermography is a conservative technique to assess the adhesive joint fatigue strength.

Regarding to fracture process, Fig. 12 shows lateral images from SP_2 in three different regions, in which the black arrow points to the adhesive-substrates interface, and Figure 13 shows the same specimen after being opened to have a global perspetive of the adhesive joint failure.

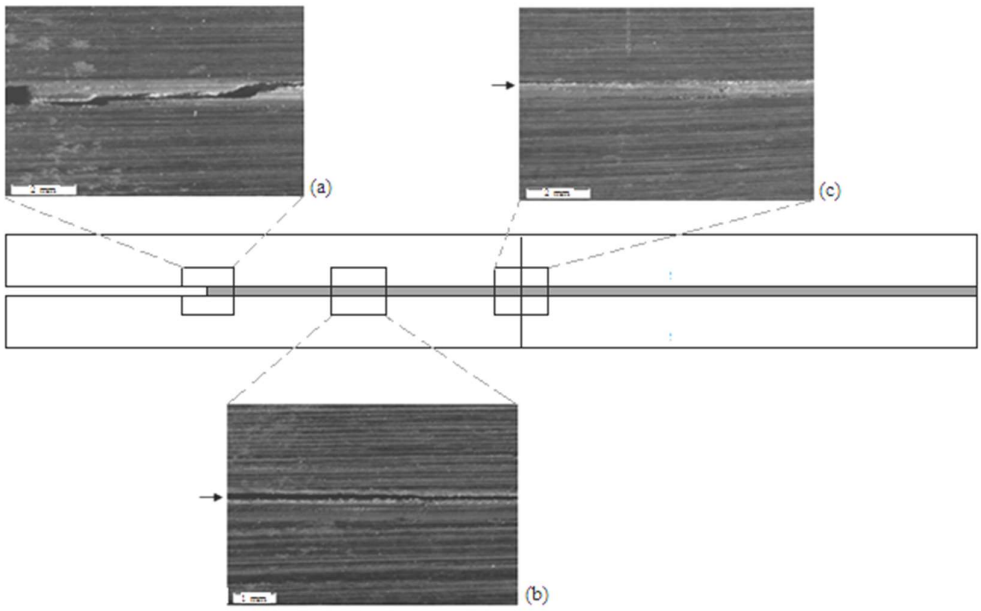

Figure 12: Failure mode of SP_2 by an optical microscope:(a) adhesive (1 X), (b) cohesive (0.63 X) (c) adhesive (1 X).

Figure 13: Specimen SP_2 opened.

The specimen was open through the utilization of wedge effect. The darker zone at left is relative to the initial crack (a_0). The intermediate zone from the end of the darker zone through half the specimen length was spent during specimen test. The right zone between the end of intermediate zone and the specimen right extremity was developed during the application of wedge effect to open the specimen in two parts.

4. CONCLUSIONS

The objective of this research was to estimate the adhesive joint fatigue strength of a bonded joint using the thermographic technique proposed by Risitano.

The results obtained for the adhesive joint fatigue strength seem to be reasonable from the technique point of view, since the relationship ΔT x Q obtained for PS_2 and PS_3 were in accordance with the expected bilinear trend behavior. In addition, the maximum value of FS is lower than the load level tested in de Barros *et al*. [14] which did not fail sand blasting specimens after reaching more than $1 \cdot 10^6$ cycles. These results confirm that the thermographic technique is quite promising as an alternative approach to estimate the bonded joint fatigue strength, in a faster and cheaper way.

REFERENCES

[1] Pereira, A.M., Ferreira, J.M., Antunes, F.V. and Bartolo, P.J. Study on the fatigue strength of AA 6082-T6 adhesive lap joints. International Journal of Adhesion and Adhesives; 2009; vol. 29; 6:633–638; https://doi.org/10.1016/j.ijadhadh.2009.02.009..

[2] Shenoy, V., Ashcroft, I.A., Critchlow, G.W. and Crocombe, A.D. Unified methodology for the prediction of the fatigue behaviour of adhesively bonded joints. International Journal of Fatigue; 2010; vol. 32;8:1278–1288; https://doi.org/10.1016/j.ijfatigue.2010.01.013.

[3] Pirondi, A. and Moroni, F. An investigation of fatigue failure prediction of adhesively bonded metal/metal joints. International Journal of Adhesion and Adhesives; 2009; vol. 29; 8:796–805; https://doi.org/10.1016/j.ijadhadh.2009.06.003.

[4] Beber, V.C., Fernandes, P.H.E., Fragato, J.E., Schneider, B. and Brede, M. Influence of plasticity on the fatigue lifetime prediction of adhesively bonded joints using the stress-life approach. Applied Adhesion Science; 2016; 4:5; https://doi.org/ 10.1186/s40563-016-0062-8.

[5] da Costa Mattos, H.S., Monteiro, A.H. and Palazzetti, R. Failure analysis of adhesively bonded joints in composite materials. Materials & Design; 2012; 33:242–247; https://doi.org/10.1016/j.matdes.2011.07.031.

[6] Costa, M., Viana, G., da Silva, L.F.M and Campilho, R.D.S.G. Environmental effect on the fatigue degradation of adhesive joints: a review. The Journal of Adhesion; 2017; 93(1–2): 127–146; http://dx.doi.org/10.1080/00218464.2016.1179117.

[7] Abdel Wahab, M.M., Fatigue in Adhesively Bonded Joints: A Review. ISRN Materials Science; 2012; Article ID 746308; 25 pages; http://dx.doi.org/10.5402/2012/746308.

[8] Chaves, F. J. P., da Silva, L. F. M., de Moura, M. F. S. F., Dillard, D. A. and Esteves, V. H. C. Fracture Mechanics Joints: A Literature Review. The Journal of Adhesion; 2014; vol.90; 12:955-992.

[9] Blackman, B.R.K., Kinloch A.J. and Paraschi ,M. The determination of the mode II adhesive fracture resistance, G_{IIC}, of structural adhesive joints: an effective crack length approach. Engineering Fracture Mechanics. 2005; vol. 72; 6:877-897; https://doi.org/10.1016/j.engfracmech.2004.08.007.

[10] Romanos, Georges, Henkel AG & Co KGaA, Global Engineering Center.Fatigue behaviour of adhesively bonded joints and its prediction using stress analysis, International Automotive Body Congress, Garching, Germany; 2015.

[11] ISO 11003-1:2001 Adhesives -- Determination of shear behaviour of structural adhesives -- Part 1: Torsion test method using butt-bonded hollow cylinders.

[12] Allen, K.W., Smith, S.M., Wake, W.C. and van Rallte, A.O., 1985. The concept of an endurance limit for adhesive joints. Int. J. Adhesion and Adhesives, 5:1, 26-32.

[13] Prot, E.M. Fatigue Testing Under Progressive Loading, A New Technique for Testing Materials, Revue de Metallurgie, 1948; 45:481–489.

[14] De Barros S., Kenedi, P.P., Ferreira, S.M., Budhe, S., Bernardino, A.J. and Souza, L.F.G. Influence of mechanical surface treatment on fatigue life of bonded joints. Journal of Adhesion, 2017; vol.93; 8:599-612; http://dx.doi.org/10.1080/00218464.2015.1122531.

[15] Risitano, A.; Risitano, G. Cumulative damage evaluation of steel using infrared thermography. Theoretical and Applied Fracture Mechanics; 2010; 54:82-90; https://doi.org/10.1016/j.tafmec.2010.10.002.

[16] ASTM D3166-99. Standard test Method for Fatigue Properties of Adhesives in Shear by Tension Loading (Metal/Metal); 1999.

[17] Fargione, G., Guidice, F., Risitano, A. The influence of the load frequency on the high cycle fatigue behaviour. Theoretical Applied and Fracture Mechanics. 2017; 88: 97-106; https://doi.org/10.1016/j.tafmec.2016.12.004.

[18] Hou, P.; Fan, J.; Guo, Q.; Guo, X. The application of the infrared thermography on titanium alloy for studying fatigue behaviour, Frattura ed Integrità Strutturale. 2014; 27: 21-27; https://doi.org/10.3221/IGF-ESIS.27.03.

[19] Monteiro, J.P.R., Campilho, R.D.S.G., Marques, E.A.S., da Silva, L.F.M. Experimental estimation of the mechanical and fracture properties of a new epoxy adhesive. Applied Adhesion Science. 2015; 3:25; https://doi.org/10.1186/s40563-015-0056-y.

[20] de Barros, S., Champaney, L., Valoroso, N. Numerical simulations of crack propagation tests in adhesive bonded joints. Latin American Journal of Solids and Structures.2012; Vol.9; 3:339-351; https://doi.org/10.1590/S1679-78252012000300002.